Nanostructured Polymer Films with Liquid Inclusions. 2. Material Morphology and Properties

Olga Kalinina and Eugenia Kumacheva*

Department of Chemistry, University of Toronto, Toronto, Ontario M5S 3H6, Canada

Received October 5, 2001; Revised Manuscript Received January 11, 2002

ABSTRACT: Three-layer core−shell latex particles with fluid cores were used for the preparation of a polymeric nanostructured material. The fluid cores were synthesized from the low glass transition temperature core-forming polymer (CFP) covalently labeled with a fluorescent dye. The CFP was encapsulated with a thin rigid shell of shell-forming polymer 1 (SFP-1). The second shell was synthesized from the shell-forming polymer 2 (SFP-2) on the surface of the bilayer particles. The specific relationship between the glass transition temperatures, T_g's, of the polymers incorporated into the core−shell particles was T_g(CFP) < T_g(SFP-2) < T_g(SFP-1). Nanocomposite polymeric films were obtained following heat processing of the arrays of core−shell particles at annealing temperature, T_g (SFP-2) < T_{ann} < T_g(SFP-1). The morphology of the nanostructured material was studied by examining the distribution of the fluorescent dye in the polymer film. Various factors providing sharp modulation in optical properties of the composite films were examined and discussed.

Introduction

Recently, regularly structured materials strongly interacting with light have attracted great interest because of their potential applications in chemical sensors, optical limiters and switches, and display devices.[1] Among different approaches to fabrication of such materials, methods employing polymer colloid particles as the building blocks are attractive for several reasons. First, highly monodipersed particles can be synthesized in the size range varying from tens of nanometers to microns. Second, significant progress has recently been achieved in organization of colloid microspheres in periodic arrays.[2] Third, these particles can be easily functionalized during synthesis and processed into a nanocomposite material by heat processing.

In the earlier papers,[3,4] we reported on a new strategy for producing nanostructured polymeric materials with periodically modulated morphology and composition. In this approach monodipersed core−shell latex particles were employed as the building blocks of the material. The compositions of the core-forming polymer (CFP) and the shell-forming polymer (SFP) were such that the glass transition temperature, T_g, of the CFP was significantly higher than the T_g of the SFP. The core−shell particles were organized in 3D ordered arrays and annealed at the temperature T_{ann} under conditions T_g(SFP) < T_{ann} < T_g(CFP). During heat processing, the SFP filled interstitial space between the particles and formed a continuous matrix. The schematics of the structural unit and the nanostructured material are shown in Figure 1A.

When the refractive indices of the CFP and SFP are close, light scattering in the nanostructured material is minimized, and the above procedure yields a transparent polymeric material. It was demonstrated that fluorescent dyes can be incorporated in either particle cores[3] or shells.[4] In this manner, a nanocomposite material with periodically modulated optical properties was produced. When the refractive indices of the CFP and SFP were close, light scattering in the nanostructured material was minimized, and the above procedure yielded a transparent polymeric material. This material showed a promising application as a medium for 3D optical bitlike data storage: each fluorescent bead could be locally photobleached, thus representing a bit of information.[5]

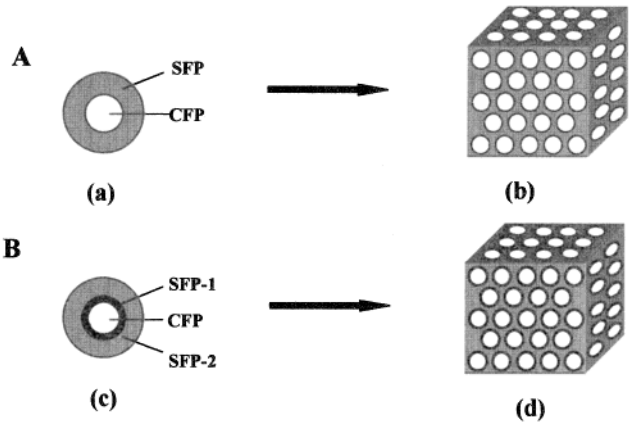

Figure 1. (A) Schematics of the "core−shell" approach to producing polymer nanocomposite materials: (a) bilayer core−shell particle with rigid core and soft shell; (b) morphology of the nanostructured material obtained using the "core−shell" approach. (B) Modified "core−shell" approach: (c) three-layer core−shell particle containing a low-T_g core, rigid shell 1, and a softer shell 2, the latter forms a matrix during heat processing; (d) morphology of the nanostructured material obtained using a modified "core−shell" approach. In the modified approach T_g(CFP) < T_g(SFP-2) < T_g(SFP-1); T_g(SFP-2) > T_{room}; T_g(CFP) < T_{room}; T_g(SFP-2) < T_{ann} < T_g(SFP-1).

Later, a modified "core−shell" approach was proposed,[6] in which the latex cores carrying a fluorescent dye were synthesized from a polymer whose T_g was significantly lower than the room temperature. The use of the low-T_g polymer was motivated by the fact that the rate of photochemical reactions carried out in polymers was significantly increased when they occurred at temperatures above the T_g of the host polymeric medium.[7] In the modified "core−shell" approach the liquid cores were first encapsulated with a thin rigid shell (shell 1); then a matrix-forming shell (shell 2) was synthesized on the surface of the SFP-1, as shown in

10.1021/ma011743n CCC: $22.00 © 2002 American Chemical Society
Published on Web 03/27/2002

Table 1. Recipes Used in Four-Stage Emulsion Polymerization of Core−Shell Particles

N stage	stage of the reaction	monomer mixture	flask content	pumping
1	synthesis of CFP	18 g BA, 12 g MMA, 0.134 g IOMP, 0.9 g EGDMA, 0.015 g NBD-MMA	70 g H_2O, 0.2 g $K_2S_2O_8$, 3 g of monomer mixture for CFP	27 g of monomer mixture for CFP
2	synthesis of SFP-1	the ingredients of monomer mixture for synthesis of SFP-1 are given in Table 2	10 g of the emulsion from stage 1 (solid content adjusted to 3 wt %)	6 g monomer mixture for SFP-1[a]
3	synthesis of SFP-2	7.5 g MMA, 7.5 g BMA, 0.067 g IOMP, 0.1 g AIBN	50 g of emulsion from the stage 2 (solid content adjusted to 3 wt %)	4 g monomer mixture for SFP-2, 4 mL of $K_2S_2O_8$ solution (c = 1 mg/mL)
4	synthesis of SFP-2	7.5 g MMA, 7.5 g BMA, 0.067 g IOMP, 0.1 g AIBN	50 g of emulsion from the stage 2 (solid content adjusted to 3 wt %)	4 g monomer mixture for SFP-2, 4 mL of $K_2S_2O_8$ solution (c = 1 mg/mL)

[a] Recipes for monomer mixtures for synthesis of SFP-1 are given in Table 2.

Figure 1c. The role of the SFP-1 in the core−shell particles was to suppress the migration of the low-T_g CFP carrying optically sensitive species into the matrix-forming polymer. It was assumed that a three-layer microsphere architecture would ensure the intactness of the liquid cores during heat processing of the material, whereas the SFP-2 would fill the interstitial voids and would form a continuous matrix.

The schematics of the three-layer particle and the polymer nanostructured material prepared using a modified "core−shell" approach are shown in Figure 1B.

In the preceding publication,[6] synthesis of the bilayer core−shell particles containing CFP and SFP-1 was described. It was demonstrated that several important parameters, such as the thickness of shell 1, the extent of cross-linking of the SFP-1, and the interfacial tension between the CFP and the SFP-1, determine monodipersity of the bilayer particles and the intactness of shell 1 during synthesis.

Here, we report on synthesis of the three-layer core−shell particles shown in Figure 1c and examine the morphology of the polymeric nanostructured material prepared using these particles. The particle cores were synthesized from the poly(methyl methacrylate) (PMMA)−poly(butyl acrylate) (PBA) copolymer. A low value of T_g of the CFP was ensured by incorporating a relatively high fraction of PBA in the latex cores. The fluid cores were encapsulated with a thin rigid shell 1 synthesized from PMMA−PBA containing a low fraction of PBA. The matrix-forming polymer, SFP-2, was synthesized from a copolymer of poly(methyl methacrylate)−poly(butyl methacrylate) (PBMA). The compositions of the CFP, SFP-1, and the SFP-2 provided the relationship T_g(CFP) < T_g(SFP-2) < T_g(SFP-1).

The main criterion in the evaluation of the modified "core−shell" approach to fabrication of photoresponsive nanocomposites was the intactness of the fluid particles in the polymer material, providing sharp periodic modulation of fluorescent properties in the ultimate material.

Experimental Section

Materials. Methyl methacrylate (MMA), butyl acrylate (BA), and butyl methacrylate (BMA) were purchased from Sigma-Aldrich Canada and purified by double distillation under reduced pressure. The initiators 2,2′-azobis(2-methylpropionitrile) (AIBN) and potassium persulfate (Aldrich, 99%), the chain-transfer agent 3-mercaptopropionic acid 2-ethylhexyl ester (IOMP, TCI America, 98%), and the cross-linking agent ethylene glycol dimethacrylate (EGDMA, Aldrich, 98%) were used as supplied. The water was purified by distillation and deionized using the Millipore Milli-Q Plus purification system. A fluorescent dye-labeled comonomer 4-amino-7-nitrobenzo-2-oxa-1,3-diazole−MMA (NBD−MMA) was synthesized as described elsewhere.[3c]

Latex Synthesis. All emulsion polymerization reactions were carried out in a three-neck flask at 80 ± 0.1 °C. The flask was equipped with a condenser, mechanical stirrer, and inlets for nitrogen and monomer. Prior to polymerization, the reaction mixture was degassed by nitrogen flow, and a small positive pressure of nitrogen was maintained during the synthesis.

The core−shell particles shown schematically in Figure 1B were synthesized by multistage emulsion polymerization using a mixed ionic−nonionic initiator approach described elsewhere.[8] A four-step synthetic procedure was used for the synthesis of the core−shell particles having a total diameter of ca. 1 μm.

In the first step, fluorescent PMMA−PBA core particles were synthesized; the weight ratio PBA/PMMA was 1.5. These particles were weakly cross-linked with 1.5 mol % EGDMA. A fluorescent dye 4-amino-7-nitrobenzo-2-oxa-1,3-diazole (NBD) was incorporated into the CFP in the amount 0.05 wt % by copolymerizing MMA−NBD with BA and MMA. The composition of the core particles remained constant in the course of experiments.

Hard nonfluorescent PBA−PMMA inner shells were polymerized on the surface of the soft latex cores in stage 2. The concentration of the cross-linking agent EGDMA in the SFP-1 was 1.5 or 9 mol. %. For each concentration of EGDMA two weight ratios PBA/PMMA (0.05 or 0.25) were examined.

The outer shell 2 was synthesized from PBMA−PMMA in the third and fourth stages. The weight ratio PBMA/PMMA in the SFP-2 was 1.0. The SFP-2 was neither cross-linked nor dye-labeled.

For the control experiment, a dispersion of the two-layer core−shell particles containing high-T_g fluorescent cores and a softer matrix-forming SFP was prepared. The CFP in these particles was synthesized from PMMA cross-linked with 1.5 mol % of EGDMA. The size of the rigid cores and the concentration of the fluorescent dye in the CFP matched the dimensions and the amount of the dye in the liquid cores in three-layer particles. Thick nonfluorescent PMMA−PBMA shells were polymerized on the surface of the rigid PMMA core particles to obtain the total microsphere size equal to the dimensions of the core−shell particles with liquid cores. The weight ratio PBMA/PMMA in the SFP-2 was 1.0.

The recipes for the latex synthesis are given in Tables 1 and 2.

Characterization of Latex Particles. After each synthetic stage particle dimensions and polydispersity index (PDI) were characterized using a photon-correlation spectroscopy (PCS) technique with Zetasizer-3000HS, Malvern Instruments, UK. In addition, morphology and dimensions of the core−shell particles were analyzed by scanning electron microscopy (Hitachi S-570 SEM) at accelerating voltage 15 kV and working distance 15 mm.

The glass transition temperatures of the CFP, SFP-1, and SFP-2 were measured on a Perkin-Elmer DSC-7 differential

Table 2. Recipes of Reaction Mixtures Used in Synthesis of SFP-1

sample	reactants
1	15 g MMA, 0.45 g EGDMA, 0.067 g IOMP, 0.1 g AIBN
2	14.25 g MMA, 0.74 g BA, 0.45 g EGDMA, 0.067 g IOMP, 0.1 g AIBN
3	12 g MMA, 3 g BA, 0.45 g EGDMA, 0.067 g IOMP, 0.1 g AIBN
4	15 g MMA, 2.67 g EGDMA, 0.067 g IOMP, 0.1 g AIBN
5	14.25 g MMA, 0.74 g BA, 2.65 g EGDMA, 0.067 g IOMP, 0.1 g AIBN
6	12.0 g MMA, 3.0 g BA, 2.55 g EGDMA, 0.067 g IOMP, 0.1 g AIBN

scanning calorimeter under a nitrogen atmosphere at a heating rate of 10 °C/min.

Polymer Film Preparation and Characterization. Dilute latex dispersions were slowly settled in Teflon containers. After removing the supernatant liquid, the sediments were dried and then annealed for 8 h at 90 °C.

The morphology of the annealed polymeric films was examined by laser confocal fluorescent microscopy (LCFM) using a BioRad MRC 600 confocal microscope with 100×/1.2 oil immersion objective lens. A 488 nm line of argon ion laser was used for excitation of the dye. For this wavelength, the vertical and the lateral resolutions of LCFM were 0.7 and 0.3 μm, respectively. The samples were imaged from the surface to approximately 200 μm below the surface.

The LCFM and SEM images were analyzed using Image Tool software (Health Science Center, University of Texas, San Antonio, TX).

Results and Discussion

Polymeric nanostructured films with fluorescent liquid inclusions were prepared in three steps which included synthesis of the core−shell particles, assembly of these particles in a periodic array, and heat processing of the arrays at the temperature exceeding the T_g of the SFP-2. Since the fluorescent dye was covalently attached to the cross-linked CFP, the localization of optically sensitive species in the liquid cores was mostly determined by the intactness of shell 1 during synthesis and annealing.[9] Both processes were carried out at elevated temperatures; heating and cooling of the core−shell particles containing polymers with different thermoexpansion coefficients could lead to rupture of the SFP-2 and release of the liquid CFP into the surroundings.[6,10,11] For this reason, the intactness of the latex particles was studied separately after synthesis and following film formation.

Latex Synthesis. Highly monodispersed fluid cores were synthesized in the first stage. The choice of the concentration 1.5 mol % of the cross-linking agent in the CFP was determined by two factors. First, the density of cross-linking of the CFP had to be sufficient to suppress diffusion of the dye-labeled polymer molecules from the latex cores to the shells. Second, the T_g of the CFP had to remain sufficiently lower than the room temperature. Fluorescent core particles with diameter 0.30 μm and PDI = 0.04, as determined by PCS, were synthesized in stage 1. The T_g of the CFP-1 in the core−shell particles was −1.6 °C.

The core particles synthesized in the first stage were used as seeds for growing rigid shells 1. The properties of the SFP-1 were varied by changing the cross-linking density. Here, we present the results obtained for two concentrations of the cross-linking agent EGDMA, C_{CLA}, in the SFP-1, that is, 1.5 and 9.0 mol %. The former value of C_{CLA} was insufficient to prevent rupture of the inner shell during synthesis and/or cooling of the latex dispersion, whereas for the higher value of 9.0 mol % the bilayer core−shell particles had a well-defined spherical shape.[6] The T_g's of the SFP-1 in the core−shell particles were 107.5 and 109.6 °C for $\phi = 0.05$ and for $C_{CLA} = 1.5$ and 9.0 mol %, respectively.

The compatibility of the CFP and the SFP-1 was varied by changing the weight ratio PBA/PMMA in the SFP-1. The experimental results in the current work are presented for $\phi = 0.05$ and $\phi = 0.25$. The former value of ϕ provided a good encapsulation of the liquid cores achieved at a relatively low volume fraction of the SFP-1 in the composite particles, whereas for $\phi = 0.25$ such encapsulation was achieved only for high volume fractions of the SFP-1 in the core−shell particles. The effect of a broader variation in C_{CLA} on particle morphology is given elsewhere.[6]

In the third and fourth consecutive stages the second matrix-forming shell was synthesized from the PBMA−PMMA copolymer on the surface of the bilayer core−shell particles. The T_g of the SFP-2 in the composite particles was 69.2 °C. The existence of the three distinct glass transition temperatures corresponding to three distinct phases in the core−shell particles gave a good indication of the structured particle morphology. The values of T_g's for the CFP, SFP-1, and SFP-2 were close to those calculated using the Fox equation[12] for the weight ratio of monomers in the reaction mixture.

In the control dispersion the size of the rigid fluorescent cores was 0. 29 μm (PDI = 0.1), and the T_g of the rigid PMMA cores was 134 °C. The matrix-forming shell was synthesized from the copolymer PBMA−PMMA, which had the same composition as the SFP-2, and the T_g = 69.8 °C. The thickness of the shell found by the SEM and PCS methods was equal to the total thickness of the inner and outer shells in the latex particles with liquid cores.

The diameters of the core−shell particles and the compositions of the CFP, SFP-1, and SFP-2 are given in Table 3.

Morphology of Nanostructured Films. After annealing the sediment of the three-layer core−shell particles, a continuous matrix was formed from the SFP-2. The films were transparent, that is, no significant light scattering was observed due to the close match of the refractive indices of the CFP, SFP-1, and SFP-2.[13] No noticeable tackiness was observed in the polymer films, indicating that no substantial release of the soft CFP in the matrix occurred during annealing.[14]

The intactness of the liquid cores in the nanostructured material was examined by studying the localization of the fluorescent dye in the domains formed by the CFP. The study was based on the fact that both the SFP-1 and the SFP-2 were optically inert. Therefore, any fluorescence from the domains other than the inclusions of the CFP originated from rupture of the SFP-1 and/or mixing of the CFP and the shell-forming polymers during annealing. The spatial variation in fluorescent intensity in the polymer nanocomposite was studied by LCFM, and it was used as a measure of dye distribution in the material.

It was anticipated that if distinct phases of the CFP, SFP-1, and SFP-2 exist in the nanostructured polymeric film and no rupture of the SFP-1 occurs, the morphology of the ultimate nanocomposite with liquid inclusions would be very similar to the control sample obtained using core−shell particles with rigid fluorescent cores.

Table 3. Compositions of CFP, SFP-1, and SFP-2 and Dimensions of Core−Shell Particles Obtained after Different Stages of Synthesis

sample	weight ratio PBA/PMMA/C_{CLA}[c] in CFP	diameter of core particles[a] [μm]	weight ratio PBA/PMMA/C_{CLA}[c] in SFP-1	diameter of two-layer core−shell particles[a] [μm]	weight ratio PBMA/PMMA in SFP-2	total diameter of core−shell particles[a] [μm]
control	0/1.5[b]	0.29			1.0	0.90
1	1.5/1.5	0.30	0/1.5	0.67	1.0	0.95
2	1.5/1.5	0.30	0.05/1.5	0.65	1.0	0.83
3	1.5/1.5	0.30	0.25/1.5	0.67	1.0	0.95
4	1.5/1.5	0.30	0/9	coagulation		
5	1.5/1.5	0.30	0.05/9	0.64	1.0	1.05
6	1.5/1.5	0.30	0.25/9	0.65	1.0	1.04

[a] Particle dimensions were measured using PCS. The standard deviation was 10 nm. [b] Core particles are synthesized from PMMA. [c] C_{CLA} is molar concentration of the cross-linking agent.

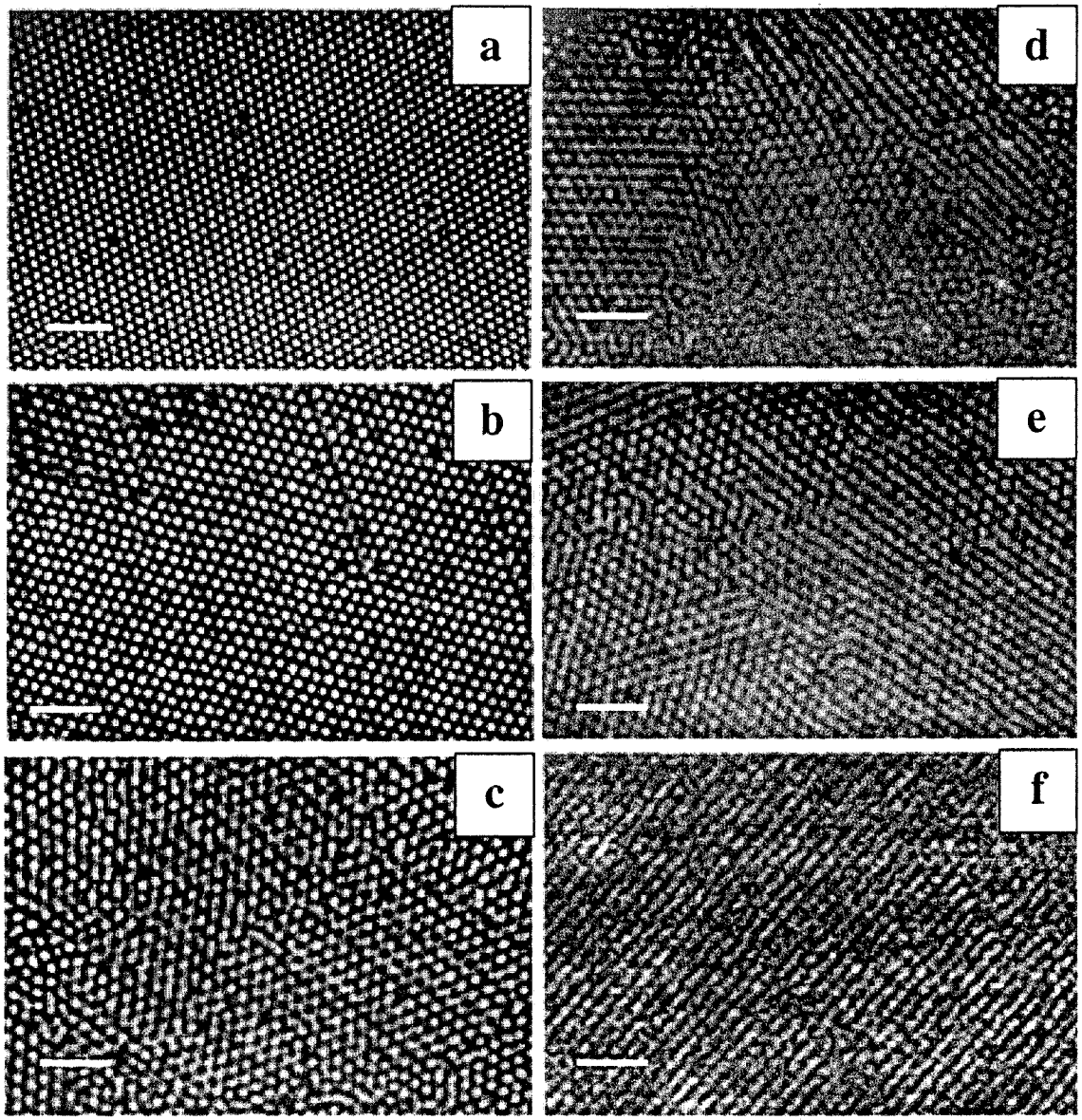

Figure 2. LCFM microphotographs of the control sample (a) and nanocomposite films with liquid inclusions prepared from dispersions 5 (b), 6 (c), 2 (d), 3 (e), and 1 (f). The composition of the dispersions is given in Tables 1 and 2. Scale bar is 5 μm. Bright domains correspond to fluorescent CFP. The position of the examined 2D slice is 10 μm below the top surface of the film.

The characteristic LCFM microphotographs of the films prepared from samples 1−6 (Table 1) are shown in Figure 2a−f. In these images, the bright domains are formed by the fluorescent CFP, whereas the black background corresponds to the optically inert domains of SFP-1 and SFP-2. First, the quality of the nanostructured films was evaluated by visual inspection of contrast between the fluorescent and nonfluorescent domains in the LCFM images. The control sample obtained from the core−shell particles with rigid PMMA cores and PMMA/PBMA shells (Figure 2a) showed the highest optical contrast between the particles and the matrix. The films obtained from dispersions 5 and 6 containing CFP with a higher degree of cross-linking

of the SFP-1 at $C_{CLA} = 9$ mol % had an optical contrast that was somewhat weaker than the control sample but notably stronger than all other films. For the same degree of cross-linking, an increase in ϕ led to a decrease in contrast in the films, as can be seen from comparing images b and c in Figure 2 obtained from latexes with $\phi = 0.05$ and 0.25, respectively.

The results of examination of the film morphology were in good agreement with the results obtained in studies of particle morphology.[6] A higher degree of cross-linking of the SFP-1 and a better compatibility between the CFP and the SFP-1 were important factors in providing good protection and integrity of the liquid cores in latex particles. For example, an insufficient degree of cross-linking led to rupture of the SFP-1 and release of the fluorescent contents of the particle cores into the surroundings;[6] this feature was further amplified during film formation and resulted in a poor optical contrast between the fluorescent and nonfluorescent domains in the film. The same effect was obtained when a somewhat poor compatibility of the CFP and the SFP-1 was observed (samples 3 and 4), although for the weight ratio SFP1/CFP of ca. 2.0 the latex cores were uniformly covered with the SFP-1.

In the next step, the distribution of the fluorescent species between the CFP, SFP-1, and SFP-2 was examined quantitatively. The nanocomposite films were studied in LCFM experiments in which the microscope settings such as brightness, contrast, intensity of sample irradiation, the number of scans, and the distance of the examined plane from the surface were the same for all films. All LCFM images were taken at the same magnification at depth 10 μm below the surface of the sample. The fact that all samples were examined at the same depth allowed us to assume that the contribution of layers other than the focal plane in sample fluorescence was the same for all films. The spatial variation of fluorescence intensity was analyzed for the control sample and for the best quality films prepared from dispersion 5 ($\phi = 0.05$, $C_{CLA} = 9$ mol %) and dispersion 6 ($\phi = 0.25$, $C_{CLA} = 9$ mol %). The morphology of these films is shown in Figure 2a−c.

The fluorescent line profiles obtained from analysis of these images are shown in Figure 3a−c, respectively. In these profiles, the distribution of the fluorescent dye between the different phases in the films is characterized by the peak-to-well height, the width of the peaks, and the average brightness of the fluorescent domains.

First, a contrast parameter, CP, was calculated as the average of 50 values of the peak-to-well heights. This parameter was equivalent to the signal-to-noise ratio in the nanocomposite film, and it gave a measure of the localization of the fluorescent dye in the particles vs the matrix. The values of the CP were 152, 135, and 71 arb.u. for the films obtained from the control latex dispersion, sample 5, and sample 6, respectively (Table 4). Thus, in the best films prepared from samples 5 and 6 the values of CP were 89% and 47% of the CP of the control film, respectively. This comparison gave additional support to the importance of a higher extent of cross-linking of the SFP-1.

Second, the average values of the peak widths measured at half-height of the peaks in Figure 3 were 0.42, 0.52, and 0.74 μm for the control film and for the films prepared from samples 5 and 6, respectively. Comparison of these values with the diameter of the core particles of 0.30 μm showed a relatively good correspondence for the control sample and a somewhat larger size of the fluorescent domains in the films with liquid inclusions. The dimensions of the fluorescent domains in films prepared from latexes 5 and 6 were 23% and 76% larger than that in the control film, whereas the size of the fluorescent cores in the core−shell latex particles was practically the same.

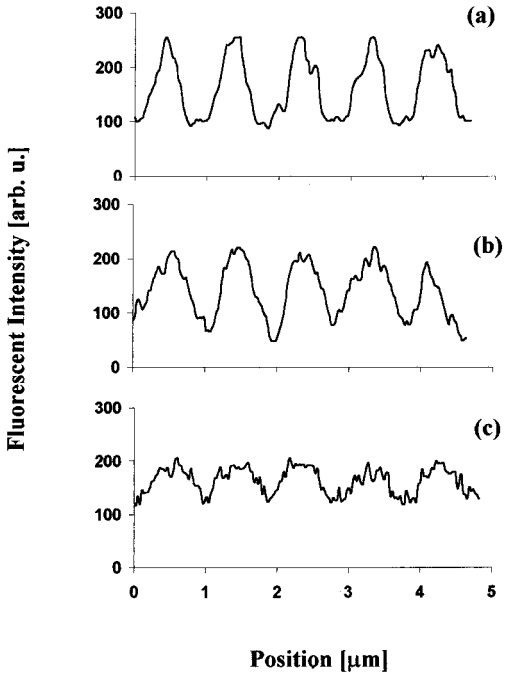

Figure 3. Spatial variation of fluorescence intensity in nanocomposite films (a), (b), and (c) shown in Figure 2.

Table 4. Results of Analysis of Spatial Variation Fluorescence Intensity Profile

sample	av width of peaks [μm]	C_{CLA}	contrast [arb.u.]	av brightness [arb.u.]
control	0.42	0	152	150
5	0.58	9	135	141
2	0.74	1.5	71	158

The third characteristic property of the nanostructured films, namely, the average brightness, was characterized by measuring the average fluorescent intensity of the material. The fluorescent intensities of 500 experimental points on line profiles a−c in Figure 3 were summed up, and the total intensity was divided by the number of points. In this manner, for the same number of peaks and wells on line profiles (that is, for the same number of fluorescent particles surrounded by the nonfluorescent matrix), the average brightness characterized fluorescence of the entire film. Since the latex cores in the control dispersion and in dispersions 5 and 6 contained the same amount of fluorescent dye, it could be anticipated that the total fluorescence intensity of the polymeric films would be the same, irrespective of the distribution of dye molecules in the film. The values of average brightness for the control sample and for the polymeric films obtained from latexes 5 and 6 were 151, 141, and 158 arb.u., respectively. These values indicated that the average fluorescence intensity was comparable for all films, despite the fact that the localization of the dye in these films was quite different.

Although the results of measurements of dimensions of fluorescent and nonfluorescent domains in the nanostructured films should be treated with caution because

of the limited resolution of LCFM, several conclusions could be made on the basis of analysis of CP and the average peak widths. First, increase in cross-linking density of the SFP-1 led to better encapsulation of the liquid inclusions, which allowed us to produce a polymeric nanostructured material with a strong modulation in fluorescent properties. The affinity of the CFP and the SFP-1 was another important factor controlling localization of the NBD dye in the core particles and a uniform encapsulation of the fluid cores with the SFP-2.[6] Second, in the nanostructured films the release of the fluorescent dye into the nonfluorescent matrix was not completely suppressed: films obtained from the control dispersion had a higher optical contrast between the particles and the matrix than films with liquid inclusions. The reason for the difference arose from partial mixing of the CFP with the SFP-1 and perhaps with the SFP-2. Another possible reason for the partial release of the CFP into the matrix could originate from microcracking of the SFP-1 during annealing.

The requirements to the SFP-2 were less demanding and included good compatibility between the SFP-1 and SFP-2 and good film-forming properties of the SFP-2.

In summary, this work has at least two important implications. First, it describes a strategy for the preparation of nanostructured optically responsive materials with fluid inclusions. The method employs the incorporation of dyes, chromophores, and possibly nonlinear optics species into the fluid cores of monodispersed core−shell latex particles. The three-layer morphology of the core−shell particles is extremely important in the fabrication of such materials, since the SFP-1 forms rigid walls confining fluid "containers" and thus suppresses the release of the fluid fluorescent CFP into the surroundings, whereas the SFP-2 forms a matrix. Second, this work demonstrates that incorporation of fluorescent dyes into fluid latex cores accompanied by studies of dye distribution in the polymer film provides a very useful tool in studies of integrity of the fluid cores in a nanocomposite material.

Acknowledgment. The authors are grateful to NSERC Canada and Nortel Networks for the financial support of this work. E.K. thanks the Ontario Government for a PREA award.

References and Notes

(1) (a) Holtz, J. H.; Asher, S. A. *Nature (London)* **1997**, *389*, 829. (b) Brzozowski, L.; Sargent, E. H. *J. Opt. Soc. B: Opt. Phys.* **2000**, *17*, 1360.

(2) (a) Rogach, A. L.; Kotov, N. A.; Koktysh, D. S.; Ostrander, J. W.; Ragoisha, G. A. *Chem. Mater.* **2000**, *12*, 2721. (b) Holdago, M.; et al. *Langmuir* **1999**, *15*, 4701. (c) Vickreva, O.; Kalinina, O.; Kumacheva, E. *Adv. Mater.* **2000**, *2*, 110. (d) Whitesides, G. M. *Adv. Mater.* **1996**, *8*, 245. (e) Jiang, P.; Bertone, J. F.; Hwang, K. S.; Colvin, V. L. *Chem. Mater.* **1999**, *11*, 2132.

(3) (a) Kumacheva, E.; Noolandi, J.; Kalinina, O. Processes and Compositions. US Patent 5952131, 09/14/99. (b) Kumacheva, E.; Kalinina, O.; Lilge, L. *Adv. Mater.* **1999**, *11*, 231. (c) Kalinina, O.; Kumacheva, E. *Macromolecules* **1999**, *32*, 4122.

(4) Kalinina, O.; Kumacheva, E. *Chem. Mater.* **2001**, *13*, 35.

(5) Siwick, B. J.; Kalinina, O.; Kumacheva, E.; Miller, D. R. J. *J. Appl. Phys.*, in press.

(6) Kalinina, O.; Kumacheva, E. *Macromolecules* **2001**, *34*, 6380.

(7) (a) Dibbern-Brunelli, D.; de Oliveira, D. G.; Atvars, T. D. Z. *J. Photochem. Photobiol. A: Chem.* **1995**, *85*, 285. (b) Talhavini, M.; Corradini, W.; Atvars, T. D. Z. *J. Photochem. Photobiol. A: Chem.* **2001**, *139*, 187.

(8) (a) O'Callagham, K. Y.; Paine, A. Y.; Rudin, A. *J. Appl. Polym. Sci.* **1995**, *58*, 2047. (b) O'Callagham, K. Y.; Paine, A. Y.; Rudin, A. *J. Polym. Sci., Part A: Polym. Chem.* **1995**, *33*, 1849.

(9) It was assumed that pressure gradients generated in the core−shell particles during heat processing and cooling are stronger than capillary pressure imposed on the microspheres during their assembly in 3D arrays.

(10) Loxley, A.; Vicent, B. *J. Colloid Interface Sci.* **1998**, *208*, 49. (b) Berg, J.; Sundberg, D.; Kronberg, B. *J. Microencapsulation* **1989**, *6*, 317.

(11) Schellenberg, C.; Akari, S.; Regenbrecht, M.; Tauer, K.; Petrat, F. M.; Antonietti, M. *Langmuir* **1999**, *15*, 1283.

(12) *Polymer Handbook*, 3rd ed.; Brandrup, J., Immergut, E. H., Eds.; Wiley: New York, 1989.

(13) The refractive indices of the CFP, SFP-1, and SFP-2 are 1.472, 1.482, and 1.485, respectively, calculated based on polymer composition and the values of refractive indices of the individual polymers, that is, $n_{PBMA} = 1.483$, $n_{PMMA} = 1.4893$, and $n_{PBA} = 1.466$.[12]

(14) Dos Santos, F. D.; Fabre, P.; Drujon, X.; Meunier, G.; Leibler, L. *J. Polym. Sci., Part B: Polym. Phys.* **2000**, *3*, 2989.

MA011743N